Journal of Controlled Release 202 (2015) 21–30

Contents lists available at ScienceDirect

Journal of Controlled Release

journal homepage: www.elsevier.com/locate/jconrel

Sonosensitive theranostic liposomes for preclinical in vivo MRI-guided visualization of doxorubicin release stimulated by pulsed low intensity non-focused ultrasound

S. Rizzitelli [a], P. Giustetto [a,b], J.C. Cutrin [a], D. Delli Castelli [a], C. Boffa [a], M. Ruzza [a], V. Menchise [c], F. Molinari [d], S. Aime [a,b], E. Terreno [a,b,*]

[a] Center for Molecular Imaging, Department of Molecular Biotechnology and Health Sciences, University of Torino, Via Nizza 52, 10126 Torino, Italy
[b] Center for Preclinical Imaging, Department of Molecular Biotechnology and Health Sciences, University of Torino, Via Ribes 5, 10010 Colleretto Giacosa (TO), Italy
[c] Institute for Biostructures and Bioimages (CNR) c/o Molecular Biotechnology Center, University of Torino, Italy
[d] Biolab, Department of Electronics and Telecommunications, Politecnico di Torino, Torino, Italy

ARTICLE INFO

Article history:
Received 29 October 2014
Accepted 23 January 2015
Available online 24 January 2015

ABSTRACT

The main goal of this study was to assess the theranostic performance of a nanomedicine able to generate MRI contrast as a response to the release from liposomes of the antitumor drug Doxorubicin triggered by the local exposure to pulsed low intensity non focused ultrasounds (pLINFU). In vitro experiments showed that Gadoteridol was an excellent imaging agent for probing the release of Doxorubicin following pLINFU stimulation. On this basis, the theranostic system was investigated in vivo on a syngeneic murine model of TS/A breast cancer. MRI offered an excellent guidance for monitoring the pLINFU-stimulated release of the drug. Moreover, it provided: i) an in vivo proof of the effective release of the liposomal content, and ii) a confirmation of the therapeutic benefits of the overall protocol. Ex vivo fluorescence microscopy indicated that the good therapeutic outcome was originated from a better diffusion of the drug in the tumor following the pLINFU stimulus. Very interestingly, the broad diffusion of the drug in the tumor stroma appeared to be mediated by the presence of the liposomes themselves. The results of this study highlighted either the great potential of US-based stimuli to safely trigger the release of a drug from its nanocarrier or the associated significant therapeutic improvement. Finally, MRI demonstrated to be a valuable technique to support chemotherapy and monitoring the outcome. Furthermore, in this specific case, the theranostic agent developed has a high clinical translatability because the MRI agent utilized is already approved for human use.

1. Introduction

The design of imaging procedures aimed at providing pharmacologists/clinicians a valuable in vivo and minimally-invasive support to visualize the effective delivery and release of a drug in the diseased region is very crucial to improve the efficiency of a pharmacological therapy and to optimize the therapeutic planning on an individual base (personalized medicine). This research area, which is part of theranosis, requires the development of chemicals that have to generate an imaging response as a function of the delivered and/or released drug [1–3]. In principle, imaging protocols for the visualization of drug delivery can be designed for almost all the available imaging modalities (nuclear, CT, optical, US, MRI, and hybrid technologies) [4–6]. However, for imaging drug release purposes, MRI is certainly the choice of election because of the widespread and successful preclinical and clinical use, the good spatio-temporal resolution, the possibility to reach deep tissues/organs without any limitations, and the rich portfolio of agents and contrast modalities available [7–9]. The motivation of using nanocarriers in the pharmacological field is mainly driven by the necessity to improve the therapeutic index of a drug. The rational is to influence the biodistribution of the drug to favor (by passive or active targeting) the accumulation and availability at the target organ, thereby improving therapeutic efficacy and reducing side effects [8,10]. However, to exert the effect, the drug needs to be released from the carrier. For the nanomedicines currently approved for clinical use, this fundamental step occurs spontaneously, i.e. following the natural degradability of the nanocarrier interacting with tissue components.

However, a significantly better control of the release can be achieved through a specific stimulation, especially suitable for treating solid

* Corresponding author at: Molecular and Preclinical Imaging Centers, Department of Molecular Biotechnology and Health Sciences, University of Torino, Via Nizza 52, 10126 Torino, Italy.
E-mail address: enzo.terreno@unito.it (E. Terreno).

http://dx.doi.org/10.1016/j.jconrel.2015.01.028
0168-3659/

tumors. Typically, triggering factors can be endogenous (chemical) or externally-applied (physical) [11–17].

The former approach consists of designing nanocarriers in which the release is controlled by biological alterations associated with the pathology (e.g. pH or overexpression of enzymes).

Alternatively, physical stimuli can be locally and selectively applied to the lesion, thereby allowing a better spatio-temporal control of the release. Among the physical stimuli, heat is certainly one of the most used. In addition to trigger the drug release, a local heating may be itself cytotoxic (e.g. hyperthermia and thermal ablation therapies) [18–20], thus synergically boosting the effect of the drug. Furthermore, it has been reported that a temperature rise can favor the extravascular accumulation of the drug due to an increase of the vascular permeability [8]. A local heating can be delivered by applying several stimuli, including high intensity focused US (HIFU), radiofrequency, magnetic fields, and microwaves [21–26].

To allow a heat-induced release, the nanocarrier system has to be suitably designed to release the drug in a narrow range of temperature, and nanotechnology offers different classes of carriers with this property (e.g. liposomes, polymeric vesicles, micelles, …) [11–13,22,25–34].

One of these systems, a temperature-sensitive liposomal formulation loaded with the anticancer drug doxorubicin, is currently in advanced clinical phase of development with the brand name of Thermodox® [35,36]. Concerning theranostic field, a MRI-detectable version of this chemotherapeutic has been already developed and tested at preclinical level [24,37,38].

Importantly, when the stimulus is applied few minutes after the i.v. administration of the nanomedicine, the blood concentration of the chemotherapeutic is maximum, thus allowing the release and the subsequent extravasation in the tumor, of a high amount of the drug. Moreover, when the released drug is a small molecule (like doxorubicin) the chemotherapeutic can diffuse into the tumor due to the increased concentration gradient between blood and tumor, and depending on the tumor penetration and clearance from the tumor. Hence, this approach can bypass the limited tumor penetration of the nanocarrier (few cell layers beyond the vessels) [6,8,39] due to the high interstitial pressure that characterizes the solid lesions.

As alternative to heat, it has been recently demonstrated that drug release can be also stimulated by using pulsed low intensity nonfocused ultrasound (pLINFU) [40–43].

pLINFU may be defined as pulsed, and non-focused acoustic waves with intensity lower than 10 W/cm^2 and US frequencies from low (20 kHz) to therapeutic (1–3 MHz) range. Hence, different to HIFU, the low energy associated with pLINFU cannot deliver enough energy to raise the temperature, and the release mechanism may primarily occur through mechanical interactions between the acoustic waves and the nanocarrier. Moreover, the low acoustic pressure applied reduces the risk of potentially unsafe cavitation effects [44–48].

In principle, pLINFU may offer some advantages over heating including: i) the extension of the triggered release to non temperature-sensitive carriers, ii) the reduction of possible toxic side effects associated with the local heating, and iii) the unnecessary control of the local temperature.

Drug release under pLINFU exposure of nanocarriers has been demonstrated in vitro in several literature reports [30–35]. Furthermore, the therapeutic benefit of this approach has been pre-clinically validated on tumor murine models [42,49,50].

MRI has been widely used to guide the delivery of nanomedicines, mostly through the incorporation of contrast agents in the surface of the carrier (e.g. the bilayered shell in case of nanovesicles) [1]. However, if the final goal is the MRI visualization of the release from nanovesicles, the best approach is certainly the encapsulation of a hydrophilic paramagnetic agent in the aqueous nanovesicle core [51,52]. In fact, the use of "MRI quenched" carriers allows the detection of a contrast enhancement when the agent (and ideally the co-encapsulated drug) is released [53–55].

Very recently, we have demonstrated that MRI can be successfully used to guide the in vivo release of the clinically approved agent Gadoteridol stimulated by tumor exposure to pLINFU [56].

In the present study, this approach has been implemented to set up a theranostic protocol in an experimental model of murine breast cancer, where MRI is used for both guiding the pLINFU-stimulated release of the anticancer drug Doxorubicin and monitoring the associated therapeutic benefit.

2. Materials and methods

2.1. Chemicals

1,2-Dipalmitoyl-sn-glycero-3-phosphocoline (DPPC), 1,2-distearoyl-sn-glycero-3-phosphocoline (DSPC), 1,2 distearoyl-sn-glycero-3-phosphoethanolamine-N-[methoxy(polyethyleneglycol)-2000]Ammonium salt (DSPE-PEG2000), and Cholesterol were purchased from Avanti Polar Inc. (Alabaster, AL, USA). Doxorubicin hydrochloride was purchased from Sigma-Aldrich (St Louise, MO, USA). Gadoteridol [Gd(HPDO3A)(H_2O)] was kindly provided by Bracco Imaging SpA (Colleretto Giacosa (TO), Italy). The culture medium RPMI 1640, the biological buffers, fetal bovine serum (FBS), glutamine, penicillin–streptomycin mixture, and trypsin were purchased from Cambrex (East Rutherford, NJ, USA).

2.2. Liposomes preparation

Theranostic liposomes (herein named Gado-Doxo-Lipo) were prepared using the method based on the hydration of a thin lipid film. Briefly, the lipid components (DPPC/DSPC/Chol/DSPE-PEG2000 at molar ratio 10:5:4:1) were dissolved in chloroform (40 mg lipid/mL). The organic solvent was removed in vacuum until a thin film was formed. Then, the film was hydrated at 55 °C with a solution of Gadoteridol 300 mM in $(NH_4)_2SO_4$ buffer 120 mM at pH 5.5. The suspension was progressively extruded at 55 °C through polycarbonate filters of decreasing pore size: 4000 nm (two times), 200 nm (two times) and 100 nm (two times). Non-encapsulated Gadoteridol was removed by exhaustive dialysis (two cycles 5 h each, 4 °C) performed against isotonic HEPES buffer (pH 7.4). Next, paramagnetic liposomes were incubated overnight (at 34 °C) with a 1 mg/mL solution of Doxorubicin, stirring continuously the suspension. Finally, the non-encapsulated Doxorubicin was removed with additional 2 dialysis cycles (5 h plus overnight) in HEPES buffer (pH 7.4, at 4 °C). Dialysis was carried out in the dark.

Additional liposomal formulations (with the same membrane composition) were prepared, containing only Gadoteridol (Gado-Lipo), only Doxorubicin (Doxo-Lipo) or none of the theranostic companions (Control-Lipo).

2.3. Liposome characterization

The mean hydrodynamic diameter of liposomes was determined using dynamic light scattering measurements (Malvern ZS Nanosizer, Malvern Instrumentation, UK) at 25 °C and a scattering angle of 90°. 10 μL of liposome suspension was diluted in 1 mL of filtered isotonic HEPES buffer (pH 7.4). Triplicate measurements were performed.

Liposomes prepared according to the procedure described above displayed a hydrodynamic diameter of 150 nm (PDI ≤ 0.1).

Gd(III) concentration (corresponding to the amount of Gadoteridol) was determined relaxometrically at 0.5 T (Stelar Spimaster, Mede (PV), Italy) measuring the longitudinal water proton relaxation rate (R_1) of the suspension after complete degradation of liposomes achieved upon addition of hydrochloric acid and concomitant heating at 180 °C [57].

Doxorubicin concentration was determined fluorimetrically (λ_{ex} = 488 nm, λ_{em} = 590 nm, Fluoromax-4 spectrofluorimeter (Horiba Jobin Yvon)) after complete degradation of liposomes with the

surfactant Triton X-100 1% v/v. Typically, the concentration of Gadoteridol in the liposome suspension was around 20 mM, while Doxorubicin concentration was around 1.8 mM (ca. 1 mg/mL). Thus, the molar ratio between encapsulated Gadoteridol and Doxorubicin was about 11:1.

2.4. US apparatus

Mice tumors were insonated with a 3.0 ± 0.1 MHz custom ultrasound transducer (designed and realized in collaboration with TEMAT s.r.l. — Torino). Piezoelectric ceramic flat disc (diameter 25 mm) transducer (STEMiNC Steiner & Martins, Inc — USA) was connected to a specific oscillator driving circuit, the circuit system used to generate the ultrasound energy in all the experiments included a tension generator (TTi EX354 RD-dual power supply 280 W), and a waveform generator (LXI KEITHLEY 3390–50 MHz) (Fig. 1). The performance of the US transducer was controlled using an oscilloscope voltage signal (Tektronix TDS1001B) with an attenuated (100×) oscilloscope probe for the connection to the circuit, and multimeter (Fluke 87 V) for the current drawn. The multimeter was inserted in series between the power generator and the oscillating circuit to monitor current absorption from operating piezoelectric component and oscilloscope (TEKTRONIX TDS 1001 B — two channel — 40 MHz 500 MS/s) at oscillatory output point to evaluated sinusoidal voltage amplitude. The piezoelectric disc was housed and fixed inside a cylinder (metal alloy ultrasound transmitter) made by two round concentric chambers. The disc was cooled down with water circulating in the external chamber. The cooling system was turned on during all the insonation time.

2.5. Experimental pLINFU setup in vitro and in vivo

The experimental insonation setup used in vitro is illustrated in Fig. 2.

The US transducer was placed in a plastic water-filled cylindrical box. The internal wall of the box was coated with an acoustic absorber sponge. The water level reached the transducer surface, so it can stabilize the temperature during the insonation time. A three-layer gel (ultrasonic gel + agar 10% + ultrasonic gel) was used as interface between the transducer and the sample. 200 μL of the liposomal sample was put in a polyethylene terephthalate container. The temperature of the sample was monitored during insonation and resulted to be unvaried at 19.6 ± 0.3 °C.

For in vivo experiments another custom 3 MHz transducer was used (acoustic intensity I = 3.3 ± 0.3 W/cm^2 and acoustic pressure P = 0.24 MPa). The tumor region was not immersed in water during pLINFU exposure. A multilayer interface composed of materials with decreasing values of acoustic impedance from tumor to transducer was designed

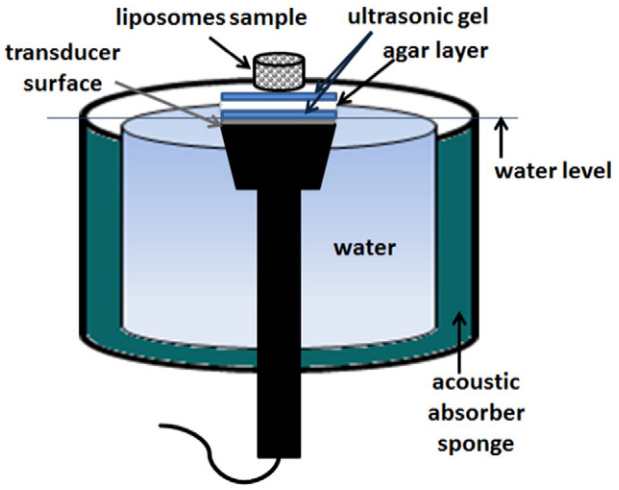

Fig. 2. Insonation setup for in vitro experiments.

(Fig. 3) to minimize backscattering effects, thus optimizing the acoustic intensity efficiency of pLINFU hitting the lesion.

2.6. Cells

TS/A cell line, derived from a spontaneous mammary adenocarcinoma which arose in a retired breeder BALB/c female [58], were cultured as monolayer at 37 °C in a 5% CO_2-containing humidified atmosphere. The culture medium was composed by: RPMI 1640 supplemented with 10% (v/v) heat-inactivated FBS, 100 IU/mL of penicillin, and 100 IU/mL of streptomycin.

2.7. Animal model

Female BALB/c mice 6 weeks-old were purchased by Charles River Laboratories and kept in standard housing (12 h light-dark cycles) with a standard rodent chow and water available ad libitum. Experiments were performed according to the national regulations and were approved by the local animal experiment ethical committee. To induce mammary adenocarcinomas, 6 × 10^5 TS/A cells were inoculated subcutaneously in the mice abdomen. The experimental protocol (schematized in Fig. 4) started one week from the cells' inoculation, when the tumor reached a volume of 40–60 mm^3. Tumor volume was determined by MRI (multislice T_{2w} images). Mice were anesthetized by intramuscular injection of tielamine/zolazepam (Zoletil®) 20 mg/kg bw and xylazine (Rompum®) 5 mg/kg bw.

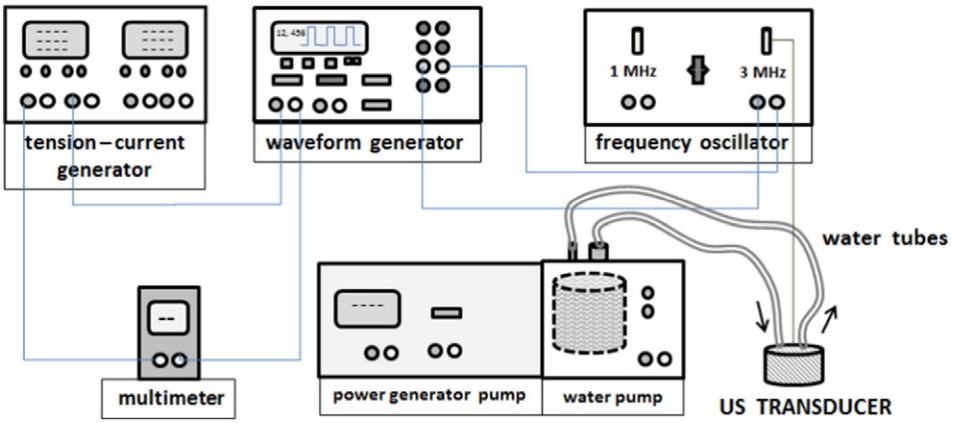

Fig. 1. Scheme of the circuit used for the generation of pLINFU.

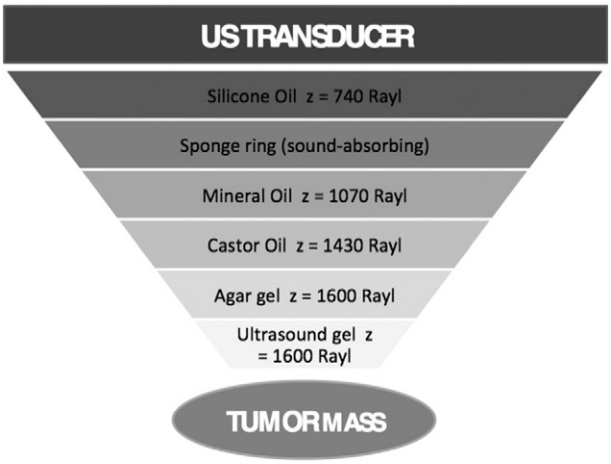

Fig. 3. Composition of the multilayer interface used for in vivo experiments.

2.8. Release experiments in vitro

Liposomes were exposed to pLINFU with different characteristics (insonation time, pulse repetition frequency (PRF)) keeping the duty cycle to 50%. After US stimulation, the sample was collected and both longitudinal water proton relaxation rate (R_1^{US}) and fluorescence were measured.

The release of Gadoteridol was determined using the following equation:

$$\text{Gadoteridol release}\,\% = \frac{R_1^{US} - R_1^{no-US}}{R_1^{Triton} - R_1^{no-US}} \cdot 100$$

where $R_1{}^{Triton}$ refers to the relaxation rate measured for the sample in which Gadoteridol was fully released through the addition of Triton X-100 (1% v/v?), and $R_1^{no\ -\ US}$ is the measurement of the sample not exposed to pLINFU.

Analogously, the release of Doxorubicin was determined using the following equation:

$$\text{Doxorubicin release}\,\% = \frac{F^{US} - F^{no-US}}{F^{Triton} - F^{no-US}} \cdot 100$$

where F^i is the fluorescence intensity of the sample.

2.9. Experimental planning

Mice enrolled in the main study were divided into three groups (n = 3 each):

- US-Group: mice injected with Gado-Doxo-Lipo (5 mg/kg bw of Doxorubicin, and 0.1 mmol/kg bw of Gadoteridol) and subjected to pLINFU exposure;
- NoUS-Group: mice injected with Gado-Doxo-Lipo (5 mg/kg bw of Doxorubicin, and 0.1 mmol/kg bw of Gadoteridol), but not subjected to pLINFU exposure;
- Control Group: mice did not receive any treatment.

Animals were anesthetized 15 min before treatment. Before each MRI session, animals were weighed and the body temperature was acquired to prevent and monitor possible changes due to side effects of the drug.

Animals were subjected to MRI (Bruker Avance 300 equipped with Micro 2.5 microimaging probe) before Gado-Doxo-Lipo injection (PRE contrast image), and repeatedly from 10 min to 90 min after liposome injection (for US-group, pLINFU exposure was carried out immediately after liposome injection). Then, additional MRI sessions at 6 h, and from day 1 to day 6 were carried out. This planning was replicated at weeks 2 and 3.

Gado-Doxo-Lipo was injected as bolus once a week for three weeks.

A single pLINFU shot (3 MHz, total insonation time 2 min, duty cycle 50%, PRF 4 Hz, 37 V), was applied to the tumors of the US-group only.

The whole protocol is summarized in Fig. 4.

Each MRI session included the acquisition of: i) a morphologic T_{2w} image (RARE sequence, TR 2000 ms, TE 3.4 ms, effective TE 27.20 ms,

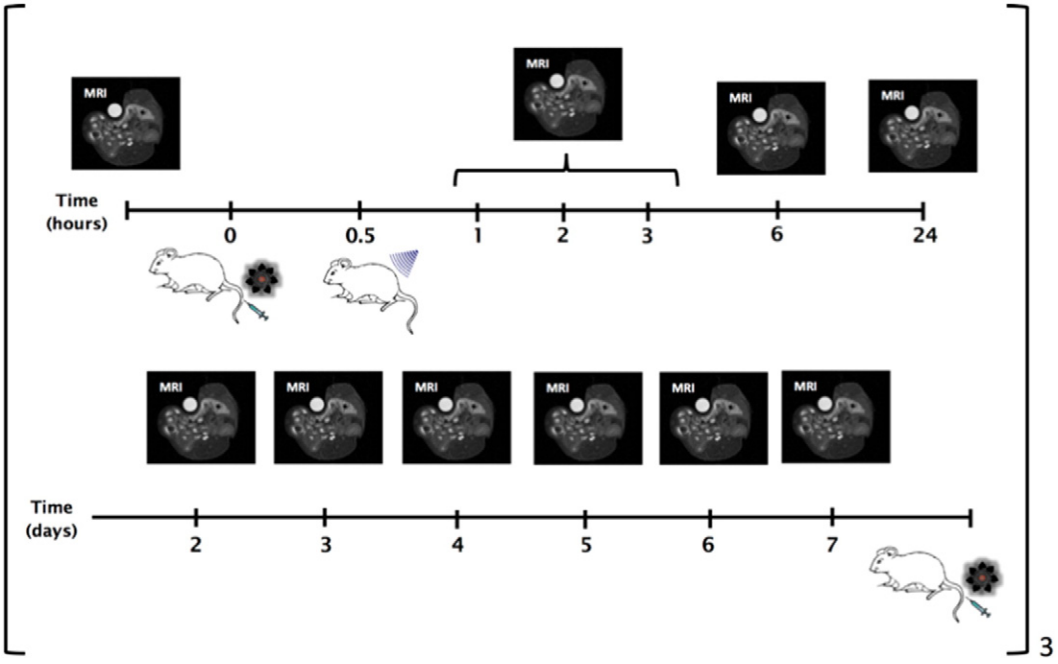

Fig. 4. Schematic view of the experimental planning. Top row: time course of the experiments in the first day. Bottom row: time course of the experiments in the first week (one MRI session per day). The overall experiments took 3 weeks for each mice enrolled in the study.

4 averages, acquisition time 1.04 min, matrix size 128 × 128, slice thickness 1 mm, FOV 3 × 3 cm), ii) a series of T_{1w} images (Multi Slice Multi Echo sequence, TR 250 ms, TE 3.2 ms, 6 averages, acquisitions time 3.12 min, matrix size 128 × 128, slice thickness 1 mm, FOV 3 × 3 cm).

T_{2w} images served to define the morphology and draw the ROI (Region of Interest) on the organs of interest (tumor, liver, spleen, kidneys, and bladder). ROIs were then transposed on T_{1w} images (acquired with the same geometry), and the T_1 Contrast-to-Noise Ratio ($CNR(T_1)$) was measured as follows:

$$CNR(T_1) = \frac{SI_{(A)} - SI_{(B)}}{SDV_{(B)}}$$

where $SI_{(A)}$ is the MRI signal intensity of a given ROI, $SI_{(B)}$ is the signal from the reference (a glass tube containing an aqueous solution of Gadoteridol) and $SDV_{(B)}$ is the standard deviation of the signal noise [59–61].

Values reported in the graphs are expressed as $CNR(T_1)$%, which correlates $CNR(T_1)$ POST-contrast to the corresponding PRE-contrast value.

2.10. Histological evaluations

Mice (n = 3) were sacrificed by cervical dislocation at different times (immediately after pLINFU application (t = 0), then 6 h and 24 h after liposomes injection). Tumors were gently removed, embedded in OCT, flash frozen in liquid nitrogen, and then stored at −80 °C until further processing. 5 μm cryosections, obtained at different depth levels of the tumor, were cut, fixed in acetone 100% for 10 min at room temperature, and preserved in the dark at 4 °C. The sections were stained with hematoxylin and eosin using a standard protocol for histological assessment of cellular density and necrosis under a light microscope (10× and 20× magnification).

2.11. Laser scanning confocal microscopy (LSCM)

Cryosections of tumors explanted from mice belonging to the experimental groups described in Section 2.10 were analyzed with Laser Scanning Confocal Microscopy (Leica TCS SP5, Leica Microsystem Srl.). Experiments were carried out using a 20× dry lens and a 63× oil-wet lens. Doxorubicin was visualized in the red channel (λ_{ex} 488 nm; λ_{em} 590 nm). Hoescht dye (Sigma-Aldrich) was added for nuclear staining and visualized in the blue channel (λ_{ex} 358 nm; λ_{em} 461 nm).

2.12. Texture analysis of the LSCM images

Texture analysis aims at numerically evaluating the smoothness, coarseness, and regularity of the pixel distribution in an image. Among all the texture descriptors that have been proposed [62], we chose the following two: Haralick's Entropy (I_{Entr}) and Haralick's Homogeneity (I_{hmg}) [63]. The Haralick features (also called second order statistical descriptors) are based on the Gray Level Co-occurrence Matrix (GLCM). Let the image be represented by a $M \times N$ gray-scale matrix $I(i, j)$, where each element of the matrix indicates the intensity of a single pixel in the image. The co-occurrence matrix $C(i,j|\Delta x, \Delta y)$ is the second-order probability function estimation that denotes the rate of occurrence of a pixel pair with gray levels i and j, given the distances between the pixels are Δx and Δy in the x and y directions, respectively. The co-occurrence matrix $C(i, j|\Delta x, \Delta y)$ can be written as

$$C(i,j|\Delta x,\Delta y) = |\{(p,q),(p+\Delta x, q+\Delta y) : I(p,q) = i, I(p+\Delta x, q+\Delta y) = j\}|$$

where $(p, q)(p + \Delta x, q + \Delta y) \in MxN$, $d = (\Delta x, \Delta y)$, and $|\cdot|$ denote the cardinality of a set. The probability that a gray level pixel i is at a distance $(\Delta x, \Delta y)$ away from the gray level pixel j is given by

$$P(i,j) = \frac{C(i,j)}{\sum C(i,j).}$$

The homogeneity I_{hmg} can be defined as:

$$I_{hmg} = \sum_{i=0}^{N-1}\sum_{j=0}^{N-1} \frac{1}{1+(i-j)^2} P(i,j)$$

and the entropy I_{Entr} as:

$$I_{Entr} = \sum_{i=0}^{N-1}\sum_{j=0}^{N-1} P(i,j)\log(P(i,j)).$$

When the image is composed of large regions having the same intensity, the probability $P(i,j)$ grows, because there are locally a lot of occurrence of pixels with the same intensity in all directions. Conversely, when the image has diffused and widespread intensities $P(i, j)$ decreases. Hence, I_{hmg} is expected to decrease as the color in the image is more and more diffused, whereas I_{Entr} is expected to increase. Homogeneity is bounded between 0 and 1, whereas entropy has a lower bound to 0 but it is not upper-bounded.

Usually, texture analysis is used to classify the morphological features of an image. We applied texture analysis to the layer colors of the histological images, with the objective of quantifying the spatial organization of the Doxorubicin. Hence, we first decomposed the color images acquired by confocal microscopy into the red, blue and, background channels by using the Ruifrock's decomposition [64]; then we applied the texture analysis to the red channel (indicative of the Doxorubicin localization).

3. Results

3.1. In vitro release

The pLINFU-stimulated release of the theranostic companions (Doxorubicin and Gadoteridol) from stealth liposomes was first tested in vitro. The percentage of release was determined as a function of PRF keeping the duty cycle constant (50%). The temperature of the sample was constantly monitored and never exceeded 34 °C, i.e. well below the gel-to-liquid phase transition temperature of the liposome bilayer (ca. 41 °C), thereby indicating that the release was not heat-mediated.

After stimulation, each sample was collected and the release of both Gadoteridol and Doxorubicin was determined by relaxometry and spectrofluorimetry, respectively.

The results confirmed the strong dependence of the release on PRF values, and, very important, highlighted the close similarity in the release of the two compounds over the entire PRF range investigated (Fig. 5). The maximum release observed in vitro (about 45%) was measured at a PRF value of 2.5 Hz. Samples not treated with pLINFU did not exhibit any release.

This finding gave a strong support to the possibility of using MRI as in vivo guidance to report the effective intratumor release of the drug after local pLINFU application.

3.2. Imaging release in vivo by MRI

Three experimental mice groups (n = 3) were enrolled in the in vivo study, but only two of them (US- and NoUS-groups) were injected with the theranostic liposomes (Gado-Doxo-Lipo).

The US-group was insonated immediately after the injection of the liposomes to maximize the amount of the released drug, and, consequently, to increase the associated MRI contrast.

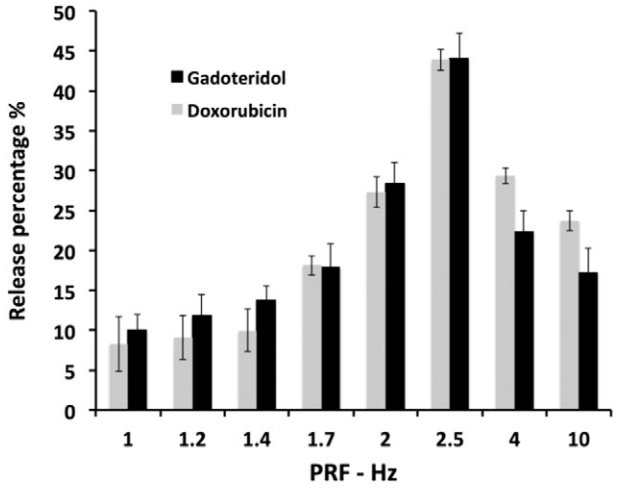

Fig. 5. pLINFU-stimulated release of Doxorubicin and Gadoteridol from stealth liposomes in vitro. The release was evaluated by spectrofluorimetry (Doxorubicin) and relaxometry (Gadoteridol), respectively. Liposomes were insonated by non-focused US, total time 2 min, duty cycle 50%.

Mice of both groups were subjected to MRI. T_1 contrast to noise ratio ($CNR(T_1)$) was consecutively measured in the tumor, liver, spleen, kidneys and bladder in the first 90 min post-injection. MR images were also longitudinally acquired after 6 h, and then daily for 7 days. This experimental scheme was replicated for three weeks (Fig. 4).

Fig. 6 reports the $CNR(T_1)$ values (expressed as percentage) measured in the tumor of the US- and NoUS-groups.

pLINFU-stimulated mice showed significantly higher $CNR(T_1)$ values than the untreated group, as expected in case of successful release of Gadoteridol. The enhancement for the US-group was maximal just after the stimulation and decreased within 6 h. Contrarily, a much smaller enhancement was detected in the NoUs-Group, which was due to the intratumor circulation of the intact "MRI-quenched" liposomes. A representative example of the MR images acquired after the injection of the liposomes is reported in the Supplementary Material (Fig. S1).

Very interestingly, after the initial decrease, $CNR(T_1)$ values slowly increased from day 1 to day 3/4 and then diminished again until the successive injection. Likely, this long-term enhancement, which was also observed for the NoUS-group, could be the consequence of the degradation of the paramagnetic liposomes internalized by tumor stroma cells

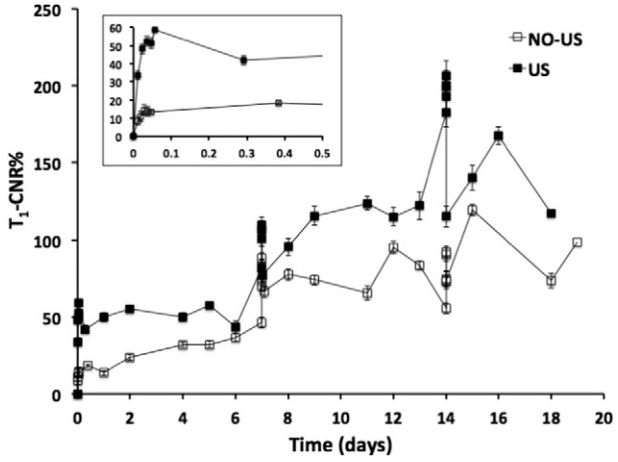

Fig. 6. Time evolution of $CNR(T_1)$% measured in the tumor for the US- and NoUS mice groups after injection of Gado-Doxo-Lipo. Liposomes were injected IV at days 0, 7 and 14 with a dose of 0.1 mmol/kg bw of Gadoteridol and 5 mg/kg bw of Doxorubicin. The inset shows the evolution after the first injection.

(mainly cancer cells and tumor associated macrophages) as already reported after the intratumor injection of Gadoteridol-loaded liposomes [65].

To support this hypothesis, a group of mice (n = 3) were injected with free Gadoteridol (that cannot be taken up by stromal cells) in the presence of Doxo-Lipo. The $CNR(T_1)$% values in the tumor were measured until 4 days after administration (no pLINFU). The T_1 contrast enhancement observed (Fig. S2) was very similar to the US-group for the first 6 h, but, then, instead of increasing, the contrast stabilized to the basal pre-injection value.

As Gadoteridol has a predominant renal excretion (blood half-lifetime of ca. 3 h in mice [50]), it is expected that the pLINFU-triggered release of the agent in the tumor is associated with the accumulation in the kidney calyx and bladder. The presence of a very bright T_1 contrast in both of these compartments (Fig. 7) just after the tumor insonation was a clear evidence of the effective intratumor release of the MRI probe triggered by the local pLINFU application.

A further indirect confirmation of the intratumor release of Gadoteridol in the US-group was gained by measuring the contrast in the liver and spleen where it is well known that liposomes rapidly accumulated after injection. The data reported in Figures S3 and S4 indicate that the $CNR(T_1)$ values measured in these organs were higher for the NoUS-group than the US-treated group. Most likely, this observation can be interpreted considering that the pLINFU exposure reduced the amount of paramagnetic liposomes circulating in the blood, thereby decreasing the liver and spleen uptake of the liposomes, with the consequent diminution of T_1 contrast.

3.3. Ex-vivo confocal microscopy

To support the results obtained in vivo by MRI, a confocal fluorescence microscopy study was carried out on tumor sections of the US- and No-US-groups explanted at different times (0, 6 and 24 h) post-injection of Gado-Doxo-Lipo. Tumors excised immediately after the pLINFU stimulation showed a diffuse fluorescence (Fig. 8 left), thereby indicating a quite homogeneous distribution of the drug into the lesion. Contrarily, images from the NoUS-group (Fig. 8 right) displayed a much more focused fluorescence, which was not detected in the necrotic. To obtain a quantitative analysis of the confocal images that could numerically assess the distribution of the fluorescent signal in the tissue, a texture analysis approach described in Section 2.12 was applied. The results are reported in Table 1 and confirmed the different distributions of the signal between the US- and NoUS-groups. We measured that the homogeneity of the image was equal to 0.56 for the NoUS-image (Fig. 8 right) and 0.46 for the US (Fig. 8 left). The entropy increased from 5.13 (NoUS) to 6.53 (US), thus documenting the more diffused distribution of the Doxorubicin after pLINFU insonation.

3.4. Insights on the release mechanism in vivo

To understand better the mechanism underlying the pLINFU-mediated extravascular diffusion of Doxorubicin in the tumor, additional experiments were carried out upon injection of the free drug with or without pLINFU exposure.

Quite surprisingly, in both cases fluorescence microscopy indicated a clear intravascular distribution of the drug (Fig. 9, left and middle), thus suggesting that the insonation alone did not affect the permeability of the tumor vasculature.

However, if free Doxorubicin was co-injected with Gadoteridol-loaded liposomes, a clear intratumor diffusion of the drug (confirmed by texture analysis, see Table 1) was observed after pLINFU stimulus (Fig. 9, right). This finding highlighted the key role played by liposomes to allow the extravasation of the released drug, thus favoring the broad diffusion in the tumor. The texture analysis confirmed the higher diffused pattern of the Doxorubicin: when Doxorubicin was co-injected with Gadoteridol-loaded liposomes and then insonated by pLINFU, the

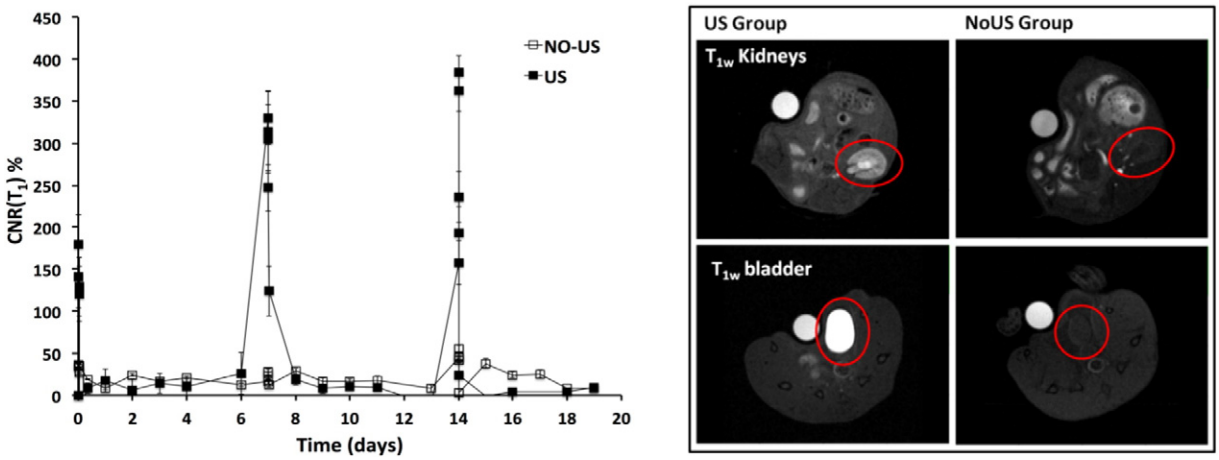

Fig. 7. Left: temporal evolution of CNR(T_1) values measured the calyx of the kidneys for the US- and NoUS-groups. Right: T_{1w} MR images of kidneys (top row) and bladder (bottom row) 15 min after liposome injection.

homogeneity was very low (0.25) and the entropy was high (8.75). When insonation was performed after injection of Doxorubicin alone, the homogeneity was 5.53 and the entropy was 0.50; when Doxorubicin was injected without any insonation, the homogeneity was 2.16 and the entropy was 0.82 (Table S1).

The effect of liposomes to mediate the permeabilization of the tumor endothelium was also demonstrated comparing the T_1 contrast enhancement of pLINFU-exposed mice injected with free Gadoteridol with or without the co-presence of liposomes. The noticeable increase in the CNR(T_1) values observed in the presence of the carrier (Fig. 10) is a clear indication of the extravasation of the paramagnetic agent.

3.5. Monitoring therapeutic efficacy by MRI

The acquisition of morphological T_{2w} MR images allowed the accurate monitoring of the tumor progression for the US-, NoUS-, and Control groups.

Fig. 11 reports the results obtained.

The treatment with the theranostic formulation significantly delayed the tumor growth, and a tumor shrinkage of ca. 50% (compared to Control) was observed after 10 days. Very importantly, the tumor exposure to pLINFU considerably improved the therapeutic outcome with an additional shrinkage (with respect to the NoUS-group) of ca. 60% after 16 days of treatment.

4. Discussion

4.1. In vitro release

The use of MRI to provide an in vivo imaging tool for the visualization of the release of Doxorubicin from liposomes requires the design of a MRI agent whose contrast is activated/modulated by the release of the drug. As reported by us and others [21,54,56,66], the encapsulation of a high amount of a hydrophilic paramagnetic Gd-complex in the aqueous cavity of liposomes allows for a significant reduction in the ability of the system to generate bright contrast in $T_{1\text{-weighted}}$ MR images. This effect is due to the slow diffusion of the water across the liposome bilayer. Consequently, when the agent is released from the carrier, the contrast switches on. As the MRI agent (here Gadoteridol) and the drug have typically different physico-chemical properties, it is fundamental to prove that the release of the first parallels that one of the second companion. As far as the pLINFU stimulation of the release is concerned, the data reported in Fig. 5 clearly indicate that the two compounds share a similar release profile as a function of the PRF value of the insonation, with a maximal release observed at 2.5 Hz.

Though quite unexpected (owing to the quite different physico-chemical properties of the two compounds), this finding is crucial for the use of Gadoteridol as imaging marker of the release of Doxorubicin. A similar result was reported for the same compounds encapsulated in

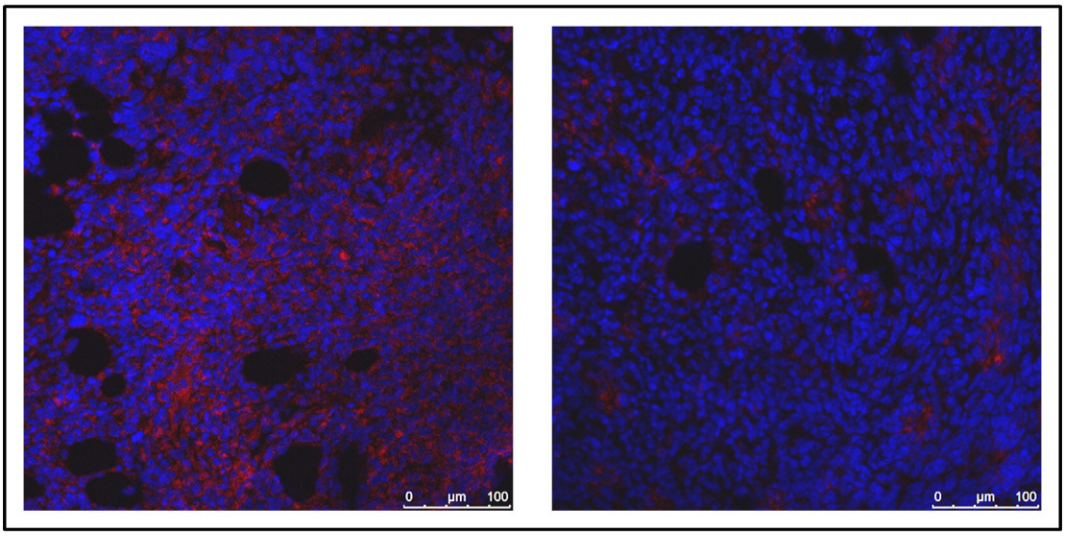

Fig. 8. CLSM images of tumor sections from the US- (left) and NoUS (right) groups explanted just after Gado-Doxo-Lipo injection. (100×, DAPI staining).

Table 1
Results of the texture analysis of the LSCM images.

Descriptor	Gado-Doxo-Lipo				
	US	NoUS	Doxo + US	Doxo − NoUS	Gado-Lipo + Doxo + US
Entropy	6.53	5.13	5.53	2.16	8.75
Homogeneity	0.46	0.56	0.50	0.82	0.25

thermosensitive liposomes and exposed to HIFU stimulus [21]. However, though the liposome formulation used in this work is expected to be temperature sensitive (DPPC has a gel-to-liquid transition temperature of ca. 41 °C), the temperature of the insonated sample never exceeded 34 °C, either in vitro or in vivo, thereby confirming that the pLINFU-controlled release was not mediated by thermal effects.

4.2. In vivo experiments

The performance of the theranostic protocol herein proposed was tested in vivo on a syngeneic mouse model of breast cancer. The tumor was induced by the subcutaneous inoculation of TS/A cells. When the tumor reached a volume ranging from 50–70 mm^3 (around 1 week post inoculation), the animals were enrolled in the study.

Three experimental groups were planned: two treated (US and NoUS) and one control.

The timeline of the experimental imaging protocol is sketched in Fig. 4 and summarized in Section 2.10.

To maximize the release of the drug in the diseased region, the pLINFU stimulus was applied: i) locally on the tumor area using a suitably developed multilayer interface to preserve as much as possible the intensity of the transmitted waves from the transducer to tumor, and ii) few minutes after the injection of the liposomes, i.e. when the amount of tumor circulating drug is the highest.

The data reported in Fig. 6 indicate that the T_1 contrast measured in the tumors of the pLINFU-treated mice was higher than the untreated group, thus suggesting the effective intratumor release of the agent from the carrier. This hypothesis was confirmed by the strong MRI signal detected in the kidneys and bladder for the treated mice only (Fig. 7), which was the consequence of the fast renal excretion of Gadoteridol.

Even the low contrast measured in liver (Fig. S3) and spleen (Fig. S4) of the treated mice is likely the result of the release of the paramagnetic agent in the tumor.

Interestingly, the observed profile in the first 24 h is slightly different from the data obtained using the same liposomal formulation (but without Doxorubicin) injected in a different tumor model (syngeneic B16.F10 melanoma) [56]. This finding is a further demonstration of how the tumor phenotype can affect the outcome of a study, thus making it very difficult to compare investigations carried out on different animal models.

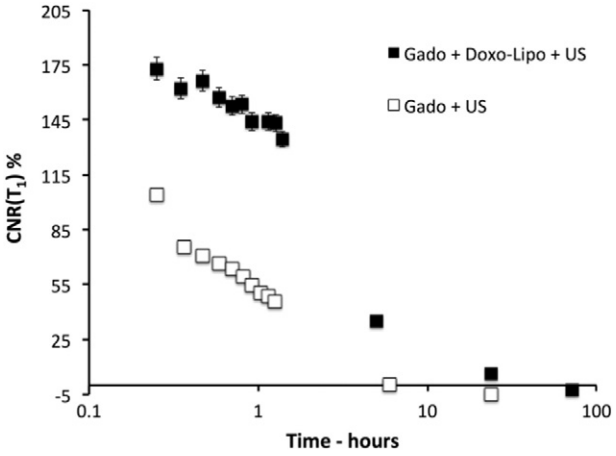

Fig. 10. Temporal evolution of CNR(T_1) values measured in the tumor area for animals treated with free Gadoteridol in the presence (filled square) or absence (open square) of liposomes, followed by pLINFU exposure.

In virtue of its fluorescence properties, the intratumor diffusion of Doxorubicin was checked by confocal fluorescence microscopy on tissue sections of explanted tumors. Importantly, pLINFU-treated tumors displayed a much more intense and diffuse fluorescence than the untreated specimens, thus indicating not only the effective stimulated release of the drug, but also the diffusion of the chemotherapeutic in the tumor stroma (Fig. 8). The higher entropy and lower homogeneity of the image corresponding to the pLINFU insonated group (Fig. 8 left) demonstrated a more diffused pattern of the Doxorubicin, that was numerically found to be more concentrated in the No-US image (Fig. 8 right).

To get more insight on the mechanisms underlying the diffusion of the drug in the lesion, additional experiments were carried out.

Interestingly, when free Doxorubicin was injected, no drug was detected in the tumor stroma in confocal microscopy images, neither after pLINFU application. In both cases, the texture descriptors were indicative of a very concentrated pattern, with low entropy and high homogeneity (Fig. 9 left and middle). This observation strongly supports the view that liposomes have an active role to allow the intratumor diffusion of the drug released in the vasculature.

A further confirmation of the role of liposomes was gained in vivo by measuring the intratumor T_1 contrast after administrating free Gadoteridol with or without co-injection of Doxo-Lipo (Fig. 10). The much higher MRI signal measured in the presence of liposomes is the

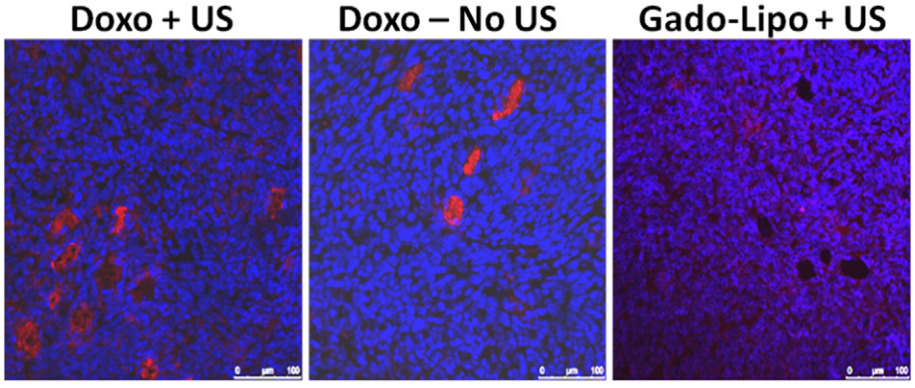

Fig. 9. CLSM images of tumor sections of mice injected with free Doxorubicin exposed (left) or not exposed (middle) to pLINFU. Right: tumor of a mouse injected with free Doxorubicin and Gadoteridol-loaded liposomes and exposed to pLINFU. Tumors were explanted just after drug administration (100×, DAPI staining).

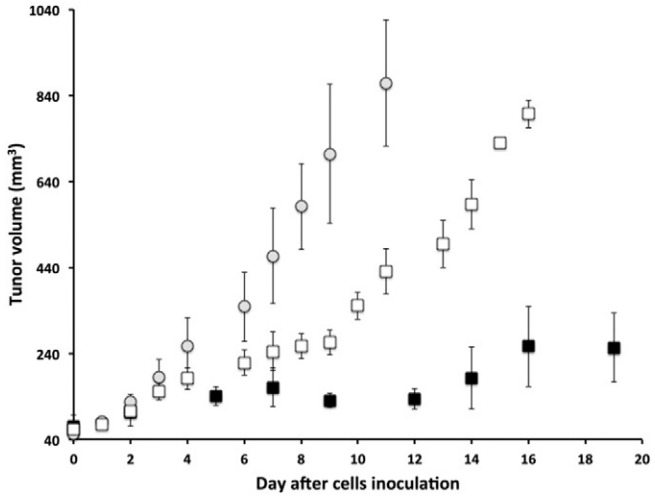

Fig. 11. Tumor progression as a function of the time elapsed from the ones monitored by MRI for the US-(filled square), NoUS (open square), and Control (gray filled circles) groups. Time zero corresponds to the moment in which the tumor volume was around 60 mm^3. Gado-Doxo-Liposomes were injected at days 0, 7, and 14. pLINFU stimulation (for US-group only) was carried out just after the injection.

consequence of the liposome/pLINFU-mediated extravasation of the MRI agent across the endothelium.

On this basis, it can be conjectured that liposomes act as a sort of acoustic resonator in the presence of pLINFU. The waves generated by the interaction between US and liposomes can induce, like sonoporation, the permeabilization of the vascular endothelium.

Interestingly, we observed similar permeabilization effects in vitro. In fact, the application of pLINFU on cells suspended in a solution containing empty liposomes and free Gadoteridol triggered the cell internalization of the MRI agent (unpublished data).

Looking at the time evolution of the T_1 contrast displayed in Fig. 5, another very interesting observation can be drawn. In both the US- and NoUS-groups, after a decrease of the contrast due to the wash out of the released Gadoteridol and the diminution of the amount of circulating paramagnetic liposomes, the contrast progressively increased reached a maximum value after 4–5 days post-injection. This delayed contrast enhancement was comparable or even higher than the CNR(T_1) values measured just after the liposome injection. As tumor stroma cells do not internalize Gadoteridol, the long-term signal enhancement is likely associated with the cellular uptake of the paramagnetic liposomes. This hypothesis was supported by the lacking of the delayed enhancement observed after the injection of free Gadoteridol (Fig. S2).

This finding is highly relevant for the clinical translation of this theranostic construct, and will deserve deep further studies that are beyond the scope of this work.

The therapeutic outcome of the theranostic protocol herein proposed was tested by measuring (by morphological MRI) the progression of the tumor volume for the US-, NoUS-, and Control-groups.

The results reported in Fig. 11 highlight the excellent performance of the pLINFU treatment that significantly delayed (starting from the second week of treatment) the tumor growth with respect to the untreated group.

5. Conclusions

This study demonstrated that MRI can successfully guide the intratumor release of Doxorubicin from liposomes stimulated by the local application of pLINFU. The method relies on the encapsulation of the clinically approved MRI agent Gadoteridol in liposomes already used in clinical chemotherapy.

This procedure provides a very valuable imaging tool to monitor the effective release of the drug in vivo on a personalized base. Furthermore, the theranostic agent investigated has a high clinical translatability. Finally, besides offering an excellent spatio-temporal guidance of the drug release process, pLINFU stimulation leads to a significant benefit in the therapeutic outcome of the chemotherapeutic, when compared with the pharmacological effect of the non-stimulated nanomedicine. Furthermore, several improvements can be envisaged like the design of systems with high ability to generate MRI contrast, the increase of the release efficiency through the optimization of the pLINFU application scheme, and the search for methods to favor the extravasation and the diffusion of the drug in the tumor.

Appendix A. Supplementary data

Supplementary data to this article can be found online at http://dx.doi.org/10.1016/j.jconrel.2015.01.028.

References

[1] E. Terreno, F. Uggeri, S. Aime, Image guided therapy: the advent of theranostic agents, J. Control. Release 161 (2) (2012) 328–337.
[2] P. Prabhu, V. Patravale, The upcoming field of theranostic nanomedicine: an overview, J. Biomed. Nanotechnol. 8 (6) (2012) 859–882.
[3] B. Sumer, J.M. Gao, Theranostic nanomedicine for cancer, Nanomedicine 3 (2) (2008) 137–140.
[4] R. Weissleder, M.J. Pittet, Imaging in the era of molecular oncology, Nature 452 (7187) (2008) 580–589.
[5] T.F. Massoud, S.S. Gambhir, Molecular imaging in living subjects: seeing fundamental biological processes in a new light, Genes Dev. 17 (5) (2003) 545–580.
[6] R. Weissleder, Molecular imaging: exploring the next frontier, Radiology 212 (3) (1999) 609–614.
[7] R.E. Jacobs, S.R. Cherry, Complementary emerging techniques: high-resolution PET and MRI, Curr. Opin. Neurobiol. 11 (5) (2001) 621–629.
[8] A.A. Manzoor, et al., Overcoming limitations in nanoparticle drug delivery: triggered, intravascular release to improve drug penetration into tumors, Cancer Res. 72 (21) (2012) 5566–5575.
[9] T. Lammers, et al., Theranostic nanomedicine, Acc. Chem. Res. 44 (10) (2011) 1029–1038.
[10] V. Torchilin, Liposomes in drug delivery, in: J. Siepmann, R.A. Siegel, M.J. Rathbone (Eds.), Fundamentals and Applications of Controlled Release Drug Delivery, Springer, New York, 2012, pp. 289–328.
[11] A.M. Ponce, et al., Hyperthermia mediated liposomal drug delivery, Int. J. Hyperth. 22 (3) (2006) 205–213.
[12] G.A. Koning, et al., Hyperthermia and thermosensitive liposomes for improved delivery of chemotherapeutic drugs to solid tumors, Pharm. Res. 27 (8) (2010) 1750–1754.
[13] D. Needham, et al., A new temperature-sensitive liposome for use with mild hyperthermia: characterization and testing in a human tumor xenograft model, Cancer Res. 60 (5) (2000) 1197–1201.
[14] E. Torres, et al., Improved paramagnetic liposomes for MRI visualization of pH triggered release, J. Control. Release 154 (2) (2011) 196–202.
[15] P. Kuppusamy, et al., Noninvasive imaging of tumor redox status and its modification by tissue glutathione levels, Cancer Res. 62 (1) (2002) 307–312.
[16] D. Mellal, A. Zumbuehl, Exit-strategies — smart ways to release phospholipid vesicle cargo, J. Mater. Chem. B 2 (3) (2014) 247–252.
[17] L. Zhu, V.P. Torchilin, Stimulus-responsive nanopreparations for tumor targeting, Integr. Biol. 5 (1) (2013) 96–107.
[18] R. Singh, S.V. Torti, Carbon nanotubes in hyperthermia therapy, Adv. Drug Deliv. Rev. 65 (15) (2013) 2045–2060.
[19] B. Bazrafshan, et al., Temperature imaging of laser-induced thermotherapy (LITT) by MRI: evaluation of different sequences in phantom, Lasers Med. Sci. 29 (1) (2014) 173–183.
[20] M. Kostrzewa, et al., Microwave ablation of osteoid osteomas using dynamic MR imaging for early treatment assessment: preliminary experience, J. Vasc. Interv. Radiol. 25 (1) (2014) 106–111.
[21] M. de Smet, et al., Magnetic resonance guided high-intensity focused ultrasound mediated hyperthermia improves the intratumoral distribution of temperature-sensitive liposomal doxorubicin, Investig. Radiol. 48 (6) (2013) 395–405.
[22] H. Grull, S. Langereis, Hyperthermia-triggered drug delivery from temperature-sensitive liposomes using MRI-guided high intensity focused ultrasound, J. Control. Release 161 (2) (2012) 317–327.
[23] A.H. Negussie, et al., Formulation and characterisation of magnetic resonance imageable thermally sensitive liposomes for use with magnetic resonance-guided high intensity focused ultrasound, Int. J. Hyperth. 27 (2) (2011) 140–155.
[24] A. Ranjan, et al., Image-guided drug delivery with magnetic resonance guided high intensity focused ultrasound and temperature sensitive liposomes in a rabbit Vx2 tumor model, J. Control. Release 158 (3) (2012) 487–494.

[25] L. Li, et al., Mild hyperthermia triggered doxorubicin release from optimized stealth thermosensitive liposomes improves intratumoral drug delivery and efficacy, J. Control. Release 168 (2) (2013) 142–150.
[26] G.M. Lanza, et al., Assessing the barriers to image-guided drug delivery, Wiley Interdiscip. Rev. Nanomed. Nanobiotechnol. 6 (1) (2014) 1–14.
[27] R. Fernando, et al., MRI-guided monitoring of thermal dose and targeted drug delivery for cancer therapy, Pharm. Res. 30 (11) (2013) 2709–2717.
[28] M.W. Dewhirst, et al., Novel Approaches to Treatment of Hepatocellular Carcinoma and Hepatic Metastases Using Thermal Ablation and Thermosensitive Liposomes, Surgical Oncology Clinics of North America 22 (3) (2013) 545–561.
[29] J.R. McDaniel, M.W. Dewhirst, A. Chilkoti, Actively targeting solid tumours with thermoresponsive drug delivery systems that respond to mild hyperthermia, Int. J. Hyperth. 29 (6) (2013) 501–510.
[30] D. Sharma, T.P. Chelvi, R. Ralhan, Thermosensitive liposomal taxol formulation: heat-mediated targeted drug delivery in murine melanoma, Melanoma Res. 8 (3) (1998) 240–244.
[31] D. Papahadjopoulos, et al., Phase transitions in phospholipid vesicles. Fluorescence polarization and permeability measurements concerning the effect of temperature and cholesterol, Biochim. Biophys. Acta 311 (3) (1973) 330–348.
[32] B.M. Dicheva, G.A. Koning, Targeted thermosensitive liposomes: an attractive novel approach for increased drug delivery to solid tumors, Expert Opin. Drug Deliv. 11 (1) (2014) 83–100.
[33] L. Li, et al., A novel two-step mild hyperthermia for advanced liposomal chemotherapy, J. Control. Release 174 (2014) 202–208.
[34] M. Nakayama, J. Akimoto, T. Okano, Polymeric micelles with stimuli-triggering systems for advanced cancer drug targeting, J. Drug Target. 22 (7) (2014) 584–599.
[35] J.P. May, S.D. Li, Hyperthermia-induced drug targeting, Expert Opin. Drug Deliv. 10 (4) (2013) 511–527.
[36] D. Needham, et al., Materials characterization of the low temperature sensitive liposome (LTSL): effects of the lipid composition (lysolipid and DSPE-PEG2000) on the thermal transition and release of doxorubicin, Faraday Discuss. 161 (2013) 515–534.
[37] S. Langereis, et al., Paramagnetic liposomes for molecular MRI and MRI-guided drug delivery, NMR Biomed. 26 (7) (2013) 728–744.
[38] S. Wang, et al., Pulsed high intensity focused ultrasound increases penetration and therapeutic efficacy of monoclonal antibodies in murine xenograft tumors, J. Control. Release 162 (1) (2012) 218–224.
[39] X.Y. Chen, S.S. Gambhlr, J. Cheon, Theranostic nanomedicine, Acc. Chem. Res. 44 (10) (2011) p. 841.
[40] C.Y. Lin, et al., Ultrasound sensitive eLiposomes containing doxorubicin for drug targeting therapy, Nanomedicine 10 (1) (2014) 67–76.
[41] H.Y. Lin, J.L. Thomas, Factors affecting responsivity of unilamellar liposomes to 20 kHz ultrasound, Langmuir 20 (15) (2004) 6100–6106.
[42] T.J. Evjen, et al., In vivo monitoring of liposomal release in tumours following ultrasound stimulation, Eur. J. Pharm. Biopharm. 84 (3) (2013) 526–531.
[43] P. Giustetto, et al., Release of a paramagnetic magnetic resonance imaging agent from liposomes triggered by low intensity non-focused ultrasound, J. Med. Imaging Health Inform. 3 (3) (2013) 356–366.
[44] S. Datta, et al., Correlation of cavitation with ultrasound enhancement of thrombolysis, Ultrasound Med. Biol. 32 (8) (2006) 1257–1267.
[45] A. Schroeder, J. Kost, Y. Barenholz, Ultrasound, liposomes, and drug delivery: principles for using ultrasound to control the release of drugs from liposomes, Chem. Phys. Lipids 162 (1–2) (2009) 1–16.
[46] A. Yudina, et al., Ultrasound-mediated intracellular drug delivery using microbubbles and temperature-sensitive liposomes, J. Control. Release 155 (3) (2011) 442–448.
[47] A. Schroeder, et al., Controlling liposomal drug release with low frequency ultrasound: mechanism and feasibility, Langmuir 23 (7) (2007) 4019–4025.
[48] M. Afadzi, et al., Mechanisms of the ultrasound-mediated intracellular delivery of liposomes and dextrans, IEEE Trans. Ultrason. Ferroelectr. Freq. Control 60 (1) (2013) 21–33.
[49] B.J. Staples, et al., Role of frequency and mechanical index in ultrasonic-enhanced chemotherapy in rats, Cancer Chemother. Pharmacol. 64 (3) (2009) 593–600.
[50] M. Knodler, et al., An analysis of toxicity in patients with recurrent and/or metastatic squamous cell carcinoma of the head and neck (R/M SCCHN) receiving cetuximab, fluorouracil and cisplatin alone or with docetaxel in a phase II clinical trial (CeFCiD), Onkologie 35 (2012) 153.
[51] H. Fattahi, et al., Magnetoliposomes as multimodal contrast agents for molecular imaging and cancer nanotheragnostics, Nanomedicine 6 (3) (2011) 529–544.
[52] S. Aime, et al., Pushing the sensitivity envelope of lanthanide-based magnetic resonance imaging (MRI) contrast agents for molecular imaging applications, Acc. Chem. Res. 42 (7) (2009) 822–831.
[53] E. Terreno, et al., Paramagnetic liposomes as innovative contrast agents for magnetic resonance (MR) molecular imaging applications, Chem. Biodivers. 5 (10) (2008) 1901–1912.
[54] S.L. Fossheim, et al., Paramagnetic liposomes as MRI contrast agents: influence of liposomal physicochemical properties on the in vitro relaxivity, Magn. Reson. Imaging 17 (1) (1999) 83–89.
[55] D.D. Castelli, et al., Metal containing nanosized systems for MR-molecular imaging applications, Coord. Chem. Rev. 252 (21–22) (2008) 2424–2443.
[56] S. Rizzitelli, P. Giustetto, C. Boffa, D. Delli Castelli, J.C. Cutrin, S. Aime, E. Terreno, In vivo MRI visualization of release from liposomes triggered by local application of pulsed low intensity non focused ultrasound, Nanomedicine 10 (5) (2014) 901–904.
[57] A. Barge, et al., How to determine free Gd and free ligand in solution of Gd chelates. A technical note, Contrast Media Mol. Imaging 1 (5) (2006) 184–188.
[58] P. Nanni, et al., TS/A: a new metastasizing cell line from a BALB/c spontaneous mammary adenocarcinoma, Clin. Exp. Metastasis 1 (4) (1983) 373–380.
[59] M.C. Steckner, B. Liu, L. Ying, A new single acquisition, two-image difference method for determining MR image SNR, Med. Phys. 36 (2) (2009) 662–671.
[60] O. Dietrich, et al., Measurement of signal-to-noise ratios in MR images: influence of multichannel coils, parallel imaging, and reconstruction filters, J. Magn. Reson. Imaging 26 (2) (2007) 375–385.
[61] R.M. Henkelman, Measurement of signal intensities in the presence of noise in mr images, Med. Phys. 12 (2) (1985) 232–233.
[62] G. Castellano, B.L., L.M. Li, F. Cendes, Texture analysis of medical images, Clin. Radiol. 59 (12) (2004) 1061–1069.
[63] R.M. Haralick, S.K., I.H. Dinstein, Textural features for image classification, IEEE Trans. Syst. Man Cybern. SMC-3 (6) (1973) 610–621.
[64] DA, R.A.a.J., Quantification of histochemical staining by color deconvolution, Anal. Quant. Cytol. Histol. 23 (4) (2001) 291–299.
[65] D. Delli Castelli, et al., In vivo MRI multicontrast kinetic analysis of the uptake and intracellular trafficking of paramagnetically labeled liposomes, J. Control. Release 144 (3) (2010) 271–279.
[66] M. de Smet, et al., Magnetic resonance imaging of high intensity focused ultrasound mediated drug delivery from temperature-sensitive liposomes: an in vivo proof-of-concept study, J. Control. Release 150 (1) (2011) 102–110.